



ELSEVIER

Contents lists available at ScienceDirect

Journal of Arrhythmia

journal homepage: [www.elsevier.com/locate/joa](http://www.elsevier.com/locate/joa)

## Original Article

# Electrophysiological and anatomical background of the fusion configuration of diastolic and presystolic Purkinje potentials in patients with verapamil-sensitive idiopathic left ventricular tachycardia



Hiroshi Taniguchi, MD<sup>a</sup>, Yoshinori Kobayashi, MD<sup>b,\*</sup>, Mitsunori Maruyama, MD<sup>c</sup>,  
Norishige Morita, MD<sup>b</sup>, Meiso Hayashi, MD<sup>a</sup>, Yasushi Miyauchi, MD<sup>a</sup>, Wataru Shimizu, MD<sup>a</sup>

<sup>a</sup> Division of Cardiology, Department of Internal Medicine, Nippon Medical School, Tokyo, Japan

<sup>b</sup> Division of Cardiology, Department of Internal Medicine, Tokai University Hachioji Hospital, 1838 Ishikawa-machi Hachioji-shi, Tokyo 192-0032, Japan

<sup>c</sup> Division of Cardiology, Department of Internal Medicine, Nippon Medical School, Chiba-Hokuso Hospital, Chiba, Japan

## ARTICLE INFO

## Article history:

Received 23 May 2014

Received in revised form

27 December 2014

Accepted 16 January 2015

Available online 24 February 2015

## Keywords:

Idiopathic left ventricular tachycardia

Verapamil-sensitive

Reentry circuit

False tendon

Purkinje potential

## ABSTRACT

**Background:** It is unclear whether false tendons (FTs) are a substantial part of the reentry circuit of verapamil-sensitive idiopathic left ventricular tachycardia (ILVT). This study aimed to prove the association between FTs and the slow conduction zone by evaluating the electro-anatomical relationship between the so-called diastolic Purkinje (Pd) potentials and FTs using an electro-anatomical mapping (EAM) system (CARTO).

**Methods:** The 1st protocol evaluated the spatial distribution of Pd and presystolic Purkinje (Pp) potentials in 6 ILVT patients using a conventional CARTO system. In the remaining 2 patients (2nd protocol), the electro-anatomical relationship between the Pd–Pp fusion potential and the septal connection of the FT was evaluated using an EAM system incorporating an intra-cardiac echo (CARTO-Sound).

**Results:** Pd potentials were observed in the posterior–posteroseptal region of the LV and had a slow conduction property, whereas Pp potentials were widely distributed in the interventricular (IV) septum. At the intersection of the 2 regions, which was located in the mid–posteroseptal area, both Pd and Pp potentials were closely spaced and often had a fused configuration. In the latter 2 patients (2nd protocol), it was confirmed that the intra-cardiac points at which the Pd–Pp fusion potential was recorded were located in the vicinity of the attachment site of the FT to the IV septum. In all patients, ILVTs were successfully eliminated by the application of radiofrequency at those points.

**Conclusion:** FTs may at least partly contribute to the formation of the Pd potential, and thus form a critical part of the reentry circuit of ILVT.

© 2015 Japanese Heart Rhythm Society. Published by Elsevier B.V. All rights reserved.

## 1. Introduction

Verapamil-sensitive idiopathic left ventricular tachycardia (ILVT) has been shown to be a clinical entity of left-sided idiopathic ventricular tachycardia (VT) [1,2]. In electrophysiological studies, two specific local potentials, the diastolic Purkinje (Pd) potential and presystolic Purkinje (Pp) potential, can be detected at the successful ablation site. The site is usually located in the left posterior septum, and these potentials are thought to be associated with the reentry circuit [3–5]. However, it remains uncertain whether these two potentials are critical for the induction and perpetuation of the tachycardia. Among these two potentials, the Pd potential is more likely to reflect a critical part of the reentry circuit

(slow conduction zone, SCZ), and has been the target of catheter ablation with successful results [3–10]. The morphology of the Pd potential has been inconsistent in previous reports, showing a relatively spiky small potential [8,9], fragmented potential [10], or small slow potentials [3–7]. These might depend on individual electrophysiological properties of the Pd substrate, defined as an anatomical structure that produces a Pd potential by its electrical excitation. Entrainment pacing during tachycardia can sometimes selectively capture the Pd potential by local stimulation [5,7]. The Pd substrate is thus believed to be of a decent size, contain cardiac muscle tissue, and be insulated from the surrounding left ventricular myocardium. The tachycardia is successfully eliminated by radiofrequency (RF) deliveries targeting the Pd potential, which is commonly located in the left posterior or posteroseptal region [1–10]. Considering the anatomical features around this region, the most likely candidate for the Pd substrate might be a false tendon (FT), which has been shown to contain working myocardium or

\* Corresponding author. Tel.: +81 42 639 1111x5002; fax: +81 42 639 1144.

E-mail address: [yoshikoba@tokai-u.jp](mailto:yoshikoba@tokai-u.jp) (Y. Kobayashi).

Table 1

Baseline data				Pd potential					Ablation site
Case no.	Age	TCL (ms)	QRS morphology	Mapping points	Size (mm)	Time (ms)	/TCL (%)	Calculated conduction velocity (m/s)	PD-QRS (ms)
<b>1st protocol</b>									
1.	32	283 <sup>a</sup>	RBBB+LAD	139	34 × 13	169	59	0.38	54
2.	39	254 <sup>a</sup>	RBBB+NW	204	35 × 14	139	54	0.25	47
3.	32	241 <sup>a</sup>	RBBB+LAD	120	39 × 17	103	42	0.20	55
4.	20	420	RBBB+LAD	162	37 × 15	270	64	0.10	50
5.	67	270 <sup>a</sup>	RBBB+LAD	106	20 × 15	150	55	0.19	63
6.	40	300 <sup>a</sup>	RBBB+NW	143	23 × 18	172	57	0.12	56
<b>2nd protocol</b>									
7.	16	300	RBBB+NW	–	–	–	–	–	60
8.	56	330	RBBB+NW	–	–	–	–	–	55
Average	38	300		146	31 × 15	167	55	0.20	55
SD	17	56		35	8 × 2	56	7	0.10	5

Time indicates the interval between the earliest to latest Pd potential.

TCL=tachycardia cycle length.

<sup>a</sup> The tachycardia could be induced during intravenous infusion of isoproterenol at 0.01–0.02 µg/m/kg.

specialized conduction tissue such as Purkinje fibers [11,12]. However, the possibility that an FT forms a substantial part of the reentry circuit is controversial [13,14]. Therefore, we evaluated the spatial distribution and activation sequence of the Pd potential using a conventional 3-dimensional (3-D) electro-anatomical mapping (EAM) system. We then targeted the latest appearance of the Pd potential, which was usually fused with the Pp potential (spiky bundle potential), in the left ventricular posteroseptal region. From the theoretical point of view, such a potential should be recorded from the exit site of the SCZ (FT-septal connection). Finally, the aim of this study was to prove the electro-anatomical relationship between the Pd–Pp fusion potential and the septal connection of the FT using a new EAM system incorporating an intra-cardiac ultrasound system.

## 2. Material and methods

### 2.1. Study population

Our study population comprised 8 patients (7 male patients, mean age: 38 ± 17 years) (Table 1) with verapamil-sensitive ILVT. None of the patients had evidence of structural heart disease on transthoracic echocardiography (TTE). The mean cycle length of the spontaneous VT was 270 ± 73 ms. The QRS morphology was a right bundle branch block (RBBB) pattern with left axis deviation in 4 patients and an RBBB pattern with a north–west axis in the remaining 4 patients, indicating a superior axis in all patients. All VTs were successfully terminated by an intravenous infusion of verapamil (3–5 mg).

### 2.2. Methods

Our study protocol was two-fold. The 1st protocol evaluated the spatial distribution of the Pd and Pp potentials and the conduction property and activation sequence of Pd potentials in 6 patients (Pts. 1–6 in Table 1). These were mapped during an induced clinical VT using the conventional EAM system. The electrophysiological study was performed after obtaining written informed consent. All anti-arrhythmic agents were discontinued for at least 3 half-lives before the study. Three multipolar electrode catheters were positioned in the right atrial appendage, right ventricular apex (RVA), and His bundle region. A 7F steerable catheter with a 4-mm electrode tip (Navi Star, Biosense Webster) was inserted via the left femoral artery and retrogradely advanced into the LV for endocardial mapping and catheter ablation. Programmed ventricular stimulation including up

to triple extrastimuli at 2 basic cycle lengths (600 ms and 400 ms) and burst pacing was applied from both the RVA and RV outflow tract to induce VT. If a sustained VT could not be induced, the programmed pacing was repeated under an intravenous infusion of isoproterenol (0.05–0.1 µg/kg/min).

#### 2.2.1. Left ventricular endocardial mapping during VT

When the induced VT was sustained, the LV was mapped using a conventional EAM system (CARTO, Biosense Webster Inc., Diamond Bar, CA, USA). The local bipolar electrogram was recorded simultaneously either with the EAM system and an EP-WorkMate (EP MedSystems Inc., Mt. Arlington, New Jersey, USA) or with a LabSystem PRO EP Recording System (Bard Electrophysiology, Lowell, Massachusetts, USA) at a filter setting of 30–500 Hz. A Pd potential was defined as a dull potential observed in the diastolic phase during VT that preceded the onset of the QRS complex by more than 40 ms (Fig. 1). On the CARTO mapping image, Pd potentials were marked with yellow dots. The conduction velocity of the SCZ was simply calculated by dividing the length between the earliest Pd site and the latest Pd site by the conduction time between these sites. The Pp potential was defined as a spiky potential observed during the presystolic phase that preceded the onset of the QRS complex by more than 0 ms (Fig. 1). Pp potentials were marked with white dots. The points at which Pd and Pp potentials were observed in proximity to one another in the same recording were marked with blue dots.

#### 2.2.2. The 2nd protocol

An additional protocol was carried out to confirm that the anatomical structure responsible for the Pd potential (Pd substrate) was the FT. EAM utilizing a new CARTO system incorporating an intracardiac echocardiogram (CARTO-Sound, Biosense Webster Inc.) was performed in the 2 most recent patients. An FT bridging from the left posterior papillary muscle to the left ventricular septum was clearly seen in each patient. We examined the local potential at the tendon–septal junction demonstrating a Pd–Pp fusion potential to clarify whether this indicated the successive activation of the false tendon and the connecting Purkinje fibers.

#### 2.2.3. Catheter ablation procedures

The target site for catheter ablation was determined according to specific local electrogram features. During endocardial mapping of the VT, we identified points at which the Pd and Pp potentials occurred in proximity to one another in the same recording

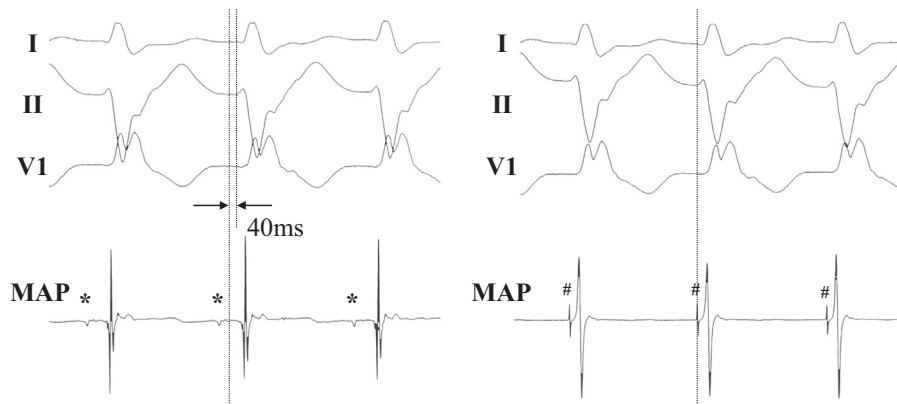


**Fig. 1.** Representative recordings of a diastolic P (Pd) potential (left panel) and presystolic P (Pp) potential (right panel). The Pd potential (marked by \*) is composed of a dull potential that precedes the onset of the QRS complex by 40 ms in this case, whereas the Pp potential (marked by #) is composed of a spiky potential observed at a time similar to the onset of the QRS complex during ventricular tachycardia (VT).

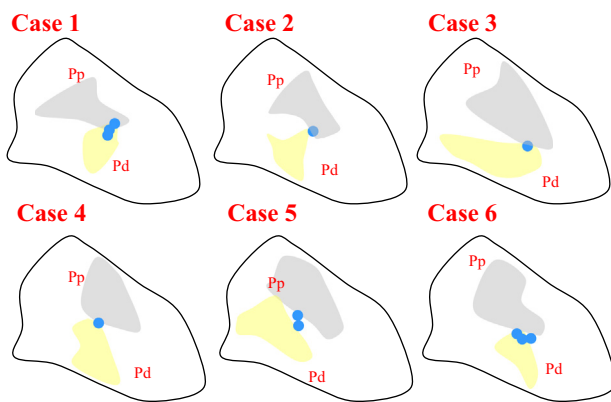


**Fig. 2.** Schematic presentation of the distribution of the Pd and Pp potentials. The gray and yellow areas indicate the respective locations at which the Pp and Pd potentials were recorded in each case. The blue dots indicate the points at which the fused Pd and Pp potentials were recorded. The abbreviations are the same as those in Fig. 1.

(tagged with blue dots in Fig. 2). Of these, the latest Pd potential, which was commonly followed by a Pp potential (Pd–Pp fusion potential), was selected for RF delivery.

RF energy was delivered using the temperature control mode set at 50–60 °C. If the tachycardia was terminated within 10 s, RF current delivery was maintained for 120 s.

#### 2.2.4. Statistical analysis

The data are presented as the mean  $\pm$  standard deviation for continuous variables and were compared using the Student *t*-test (unpaired). A *p*-value of  $<0.05$  was considered statistically significant.

### 3. Results

#### 3.1. Electrophysiological characteristics and spatial distribution of the Pd and Pp potentials (1st protocol)

In the 6 patients participating in the 1st protocol, sustained VT was induced and EAM with a mean of  $146 \pm 35$  sampling points was constructed using the CARTO system. A Pp was found in the vicinity of the infero-mid to anterior septal region and the distribution exhibited an almost similar pattern in all cases (Fig. 2). The square measure of the positive Pp potential was  $35 \pm 7 \text{ mm} \times 27 \pm 12 \text{ mm}$ . The activation sequence of the Pp

potential proceeded from the apical to basal septum during VT in all patients.

By contrast, the distribution of the Pd potential was somewhat more inconsistent. The Pd potential was observed around the middle aspect of the posterior–posteroseptal LV in Cases 1, 2, 4, and 6, but was recorded at the posterior–posteroseptal LV with a more basal extension in Cases 3 and 5 (Fig. 2). The square measure of the positive Pd potential was  $31 \pm 7 \text{ mm} \times 15 \pm 2 \text{ mm}$ . The activation sequence of the Pd potential was posterior to posteroseptal in the former 4 patients (a rather transverse direction) and basal to apical in the latter 2 patients (a rather longitudinal direction).

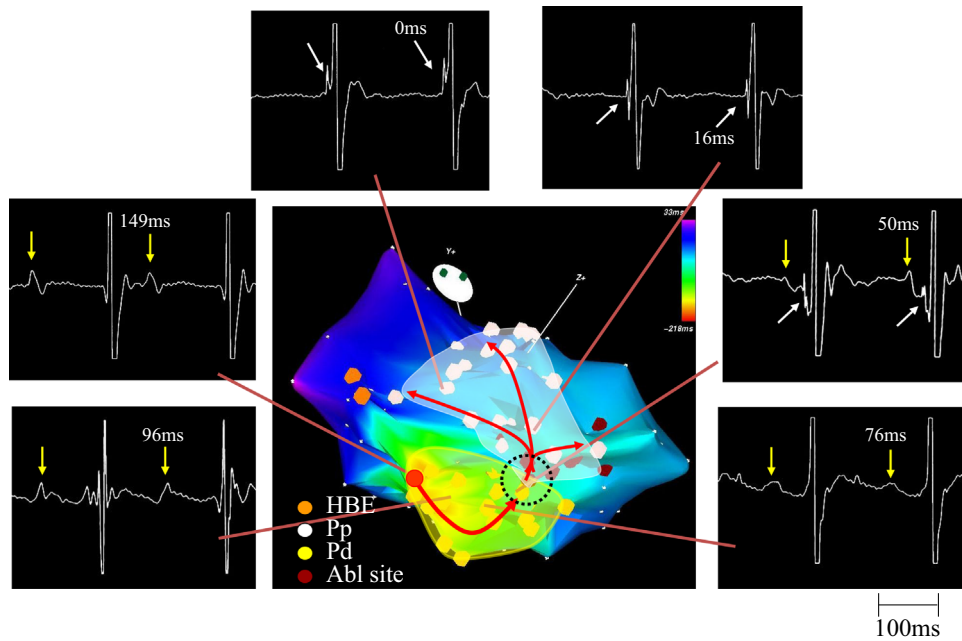
It is notable that the latest Pd and earliest Pp potentials were invariably recorded in proximity to one other even though each was widely observed in the LV. As a result, both the Pd and Pp potentials were recorded at the junction point between the Pd and Pp areas that was located in the middle aspect of the posterior septum in all patients.

The electrophysiological characteristics of the Pd potentials are summarized in Table 1. The total span (period) of the Pd potentials was  $167 \pm 56 \text{ ms}$  during the VT and was equal to  $55 \pm 7\%$  of the tachycardia cycle length. Thus, the presumed conduction velocity of the Pd was 0.20 m/s.

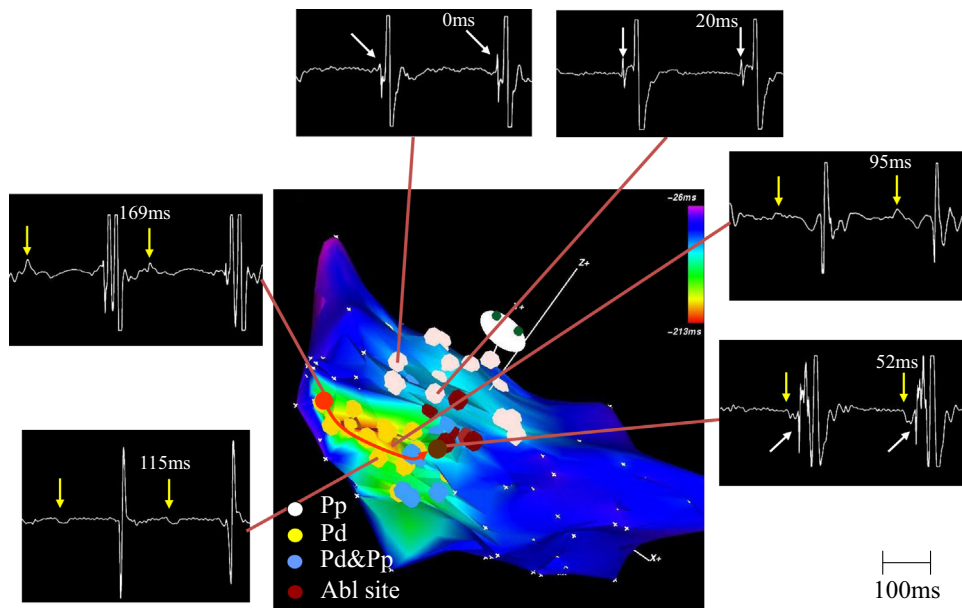
#### 3.2. Case examples

Fig. 3 shows the spatial distribution of the Pd (yellow shadow) and Pp (white shadow) potentials as well as actual intracardiac recordings of the Pd and Pp potentials in a representative case (Case 3). As marked by the yellow arrows on the local electrograms and the red arrow on the EAM image, the Pd potential appears to have conducted from the base to the apical region in the LV inferior area. Then, Pd excitation ended at a point of contact between the Pd region (yellow zone) and Pp region (white zone), where the Pd potential was immediately followed by the Pp potential (Pd–Pp fusion potential) (black dotted circle). Pp excitation then rapidly propagated toward the basal areas. Several RF current applications in the vicinity of the Pd–Pp fusion points (brown dots) rendered the tachycardia noninducible.

Fig. 4 depicts another representative case (Case 2). In contrast to the previous case, the Pd potential originates at the mid-posterior wall and proceeds toward the posteroseptal area perpendicularly to the axis of the LV rather than in the parallel direction. Pd excitation similarly ended at a point of contact between the Pd and Pp regions, at which the Pd–Pp fusion potential was observed (brown dot). The distribution of the Pp potential was similarly observed in the inter-ventricular (IV) septum. An RF energy application at the Pd–Pp fusion



**Fig. 3.** Spatial distribution of the Pd (yellow shadow) and Pp (white shadow) potentials (center panel) and the actual intracardiac recordings of the Pd and Pp potentials in Case 3. Each local electrogram was recorded at the point indicated by the brown lines. Ventricular activation mapping was performed by plotting the earliest activation time of each mapping point including Pd potentials, Pp potentials, and the ventricular wave. In this case, the earliest Pd corresponded to the earliest ventricular activation (red color). If the local electrogram contained only a ventricular wave, the onset of the ventricular wave was plotted as the activation time (blue and purple colors). For details, refer to the text.



**Fig. 4.** Spatial distributions of the Pd (yellow dots) and Pp (white dots) potentials (center panel) and actual intracardiac recordings of the Pd and Pp potentials in Case 2. Each local electrogram was recorded at the point indicated by the brown lines. Ventricular activation mapping was performed by plotting the earliest activation time of each mapping point including Pd potentials, Pp potentials, and the ventricular wave. In this case, the earliest Pd corresponded to the earliest ventricular activation (red color). If the local electrogram contained only a ventricular wave, the onset of the ventricular wave was plotted as the activation time (blue and purple colors). For details, refer to the text.

site terminated the tachycardia within 3 s (Fig. 5). Thereafter, the tachycardia was no longer inducible.

### 3.3. Anatomical background of the Pd–Pp fusion potential (2nd protocol)

The anatomical structure of the points at which the Pd–Pp fusion potential was observed was evaluated in another 2 patients with ILVT using the CARTO-Sound system. In both patients, a

fascicular structure bridging the body of the posterior papillary muscle (PPM) and infero-medial aspect of the LV septum was observed. This fascicle remained unsettled inside the LV cavity, and was thus considered to be an FT. As shown in Fig. 6, the intracardiac echo clearly displays a fascicular structure running from the PPM toward the LV septum (left lower panel). When the 3-D structure was constructed using intracardiac echo data, it became apparent that this fascicle was attached to the middle aspect of the posterior septum, as marked by the orange line



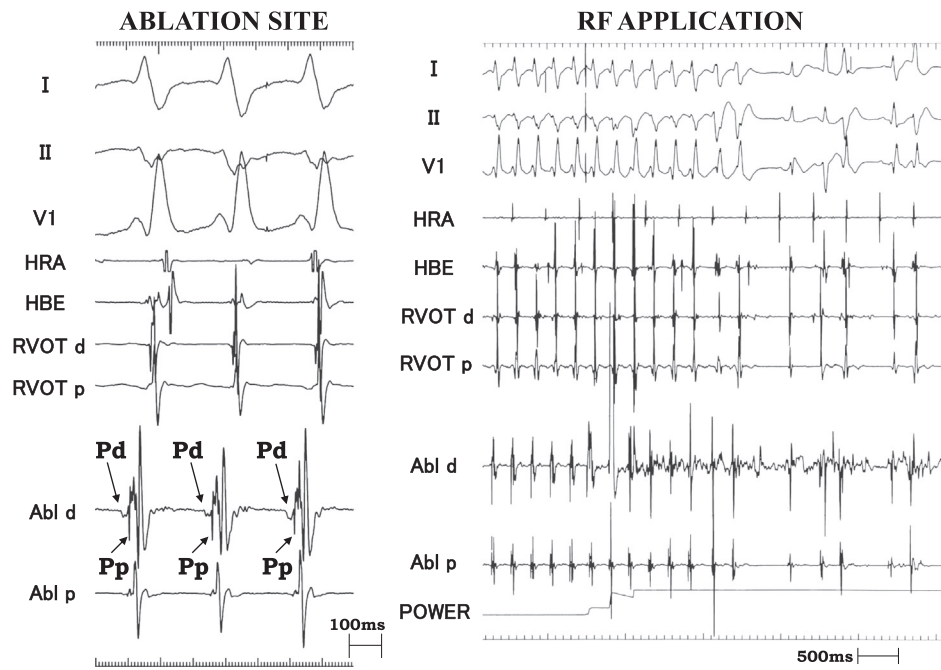


**Fig. 5.** The local electrogram at the successful ablation site shows a fused potential consisting of Pd and Pp potentials (arrows) during tachycardia (left panel), and corresponds to the local potential boxed in red in Fig. 4. An application of RF current at that point successfully terminated the VT within 2 s (right panel). From the top: surface ECG leads (lead I, II, and V1), intracardiac recordings from the high right atrium (HRA), His bundle region (HBE), right ventricular outflow tract (RVOT), and LV posteroseptal area (Abl).

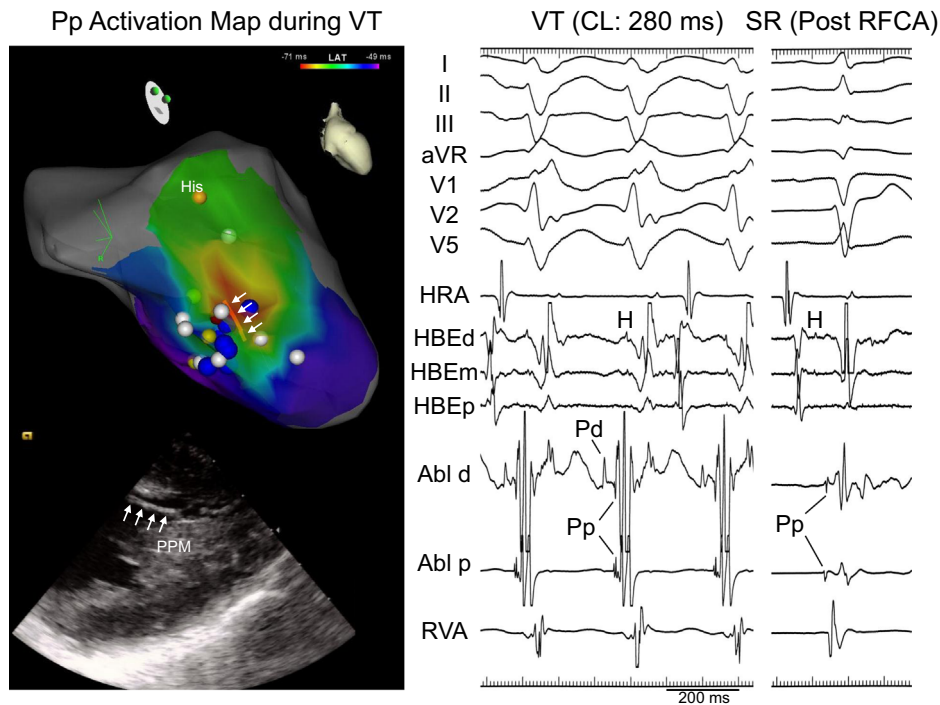


**Fig. 6.** Left upper panel: Activation map of the Pp potential during VT and 3-D location of the false tendon (white arrows: the uppermost arrow indicates the attachment site of the false tendon to the septum) running between the PPM and LV septum depicted by the CARTO-Sound system (right anterior oblique caudal views). Left lower panel: A fascicular structure runs from the PPM toward the LV septum, as shown by intracardiac echo. Near the interface of the false tendon with the LV septum, a fused potential consisting of the Pd and Pp potentials is recognized (Abl-d in the mid-panel). After spontaneous conversion to sinus rhythm, only the Pp potential can be seen (right panel). For details, refer to the text.

(left upper panel). At that point, the local electrogram exhibited both a Pd and Pp potential during VT, and the Pd potential preceded the QRS complex by 50 ms and was immediately followed by the Pp potential (fused Pd–Pp potential) (right panel). It is noteworthy that the earliest activation site of the Pp potential was located in very close proximity to the tendon–LV septal junction (left upper panel).

Based on these findings, it was inferred that the Pd–Pp fusion potential may have reflected the excitation of the exit of slow conduction, i.e., the junction of the SCZ (most likely the FT) and Purkinje fiber derived from the posterior left bundle branch. The tachycardia was terminated by RF current delivery and rendered noninducible. We confirmed almost similar electro-anatomical

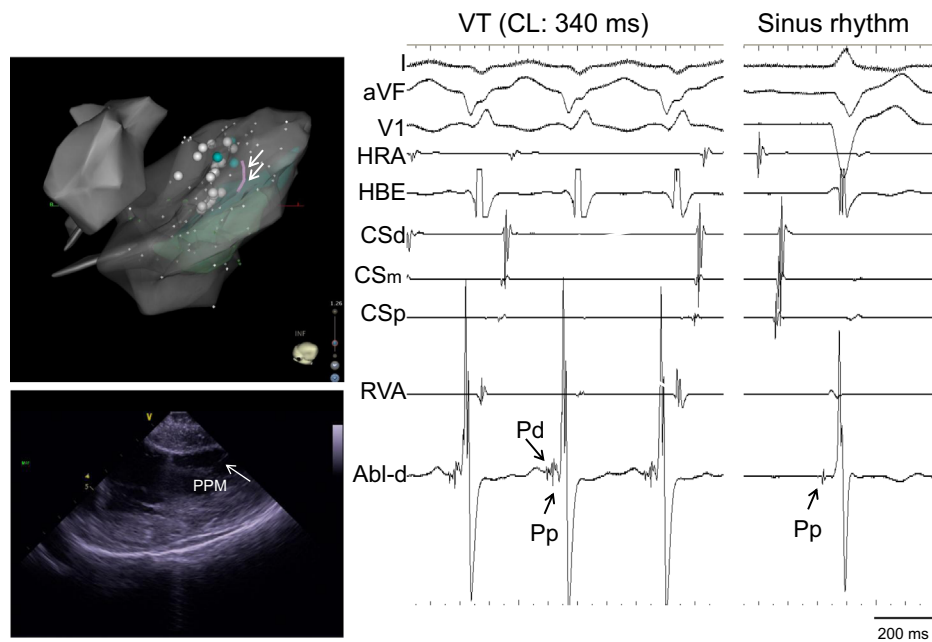


**Fig. 7.** Left upper panel: 3-D location of a false tendon observed by the CARTO-Sound system (inferior view). This false tendon also runs from the PPM to the LV septum. The brown dots indicate points at which Pp potentials were recorded and the blue dots indicate points at which Pd–Pp fusion potentials could be recorded, as shown in the mid-panel (Abl-d). It is noted that the blue dots were located in the vicinity of the interface of the false tendon with the LV septum.

findings in another patient with ILVT (Fig. 7). A Pd–Pp fusion potential could be recorded in the vicinity of the connection site of the FT at the LV septum (blue dots), and the VT was successfully eliminated by RF energy applied at that point.

## 4. Discussion

### 4.1. Major findings

The major findings of the present study are as follows. (1) The conventional EAM study conducted during tachycardia revealed a Pd potential in the posterior–posteroseptal LV, even though its distribution exhibited some degree of inter-individual variation. The activation sequence was posterior to posteroseptal (transverse direction) in 4 patients and basal to apical (longitudinal direction) in the remaining 2 patients. However, the presumed exit site of the SCZ was located in the middle aspect of the posterior septum in all patients and was immediately followed by a Pp potential (Pd–Pp fusion potential). (2) The application of the more sophisticated EAM using CARTO-Sound to 2 patients revealed that the exit site of the SCZ (the latest Pd potential fused with the Pp potential) was consistent with the site of attachment of the FT to the LV septum.

### 4.2. Electrophysiological characteristics of the Pd potential

EAM was performed during the induced tachycardia in all patients as part of the 1st protocol. Because a sustained stable ILVT could be induced only during an intravenous infusion of isoproterenol, the tachycardia cycle length was relatively short compared to that in previous reports. All tachycardias had an RBBB configuration with a superior axis, which was consistent with the previously documented tachycardias. On local electrograms, the Pd potentials were appreciable specifically in the middle level of the posterior septum that exhibited a slow conduction property. The activation time between the earliest and latest Pd potentials was equal to approximately 55% of the VT cycle length. These electro-anatomical findings regarding the Pd potential were almost consistent with previously reported findings [8,9]. Because some

periods of the tachycardia cycle were not assessed by the time of the Pd potential, we could not depict the actual entrance site of the SCZ. However, considering the data on the distribution and activation sequence of the Pd potential, it is likely that the entrance site is located more basal or more posterior to the left ventricle.

### 4.3. What is the Pd substrate?

The issue of whether the so-called FT is associated with the reentry circuit of ILVT has been controversial, and to the best of our knowledge it remains unclear [13,14]. The FT has been variously referred to as a moderator band, fibromuscular band, or merely as a muscular band. It has been shown to contain either working myocardium [11] or specialized conduction tissue with nutrition-supplying arteries [12]. Leutmer et al. [15] investigated the anatomical location of FTs in 483 consecutive autopsy cases. Among these, a total of 414 FTs were identified in 265 cases (55%). The majority (66%) of these FTs were bridging the PPM and IV septum at various levels between the base and apex of the LV. This spatial location is consistent with the spatial distribution of the Pd potential in the present ILVT cases (Fig. 2). The FT has also been shown to have complex anatomical features such as multiple tendons with a parallel and ramification (net-like) structure, which may give rise to a wide distribution of Pd potentials in some patients. This might also explain the existence of some bystander Pd potentials not involved in the tachycardia mechanism.

In some previous studies [5,6,8,9,16], the origin of the Pd potential was speculated to be the distal portion of the Purkinje fibers (Purkinje network), which are considered to possess a congenital or acquired slow conduction property. The second candidate for the Pd substrate was the FT [3,4,7,17], even though the electro-anatomical correlation between the Pd potential and Pd substrate has not been firmly established. Another possible Pd substrate is the PPM, where similar double potentials originating from the surface of the Purkinje fiber and papillary muscle tissue, were observed in some experimental studies [18,19]. However, the application of this hypothesis to the Pd and Pp potentials observed in clinical ILVT appears unreasonable, because most tachycardias

can be eliminated by RF delivery to the middle aspect of the posterior septum, which is actually remote from the anatomical location of the PPM. In our study (2nd protocol), the exit site of the SCZ, i.e., the site of the latest Pd potential immediately followed by a Pp potential (turn-around point), was located exactly at the attachment point of the FT to the LV septum, and this was confirmed by the CARTO-Sound system. This might be additional evidence in support of the idea that the FT contributes at least in part to the formation of the Pd potential, and thus forms a critical part of the reentry circuit.

#### 4.4. Optimal site for catheter ablation

We hypothesized the latest Pd potential may reflect the exit site of the SCZ, which was the most peripheral part of the reentry circuit and specialized conduction tissue. Ouyang et al. demonstrated that the earliest retrograde Purkinje potential (retro PP) observed during sinus rhythm was critical for ILVT and can be used to guide successful catheter ablation [8]. The retro PPs are usually appreciable on the mid-inferior septum and are likely to correspond to the Pd potential during VT [7]. Kaneko et al. [20] reported that such retro PPs were commonly recorded even in patients without ILVT. Although the previous studies that used EAM during ILVT depicted a linear activation of Pd potentials in the LV septum as the proposed critical conduction pathway [8,9], our study revealed that the Pd potentials were noted in a certain area in the LV septal and posterior region during ILVT. This may indicate that bystander Pd potentials are also present in the LV septum during ILVT. Because it is rarely possible to discriminate between critical and bystander Pd potentials using techniques such as entrainment pacing, simply targeting the Pd potentials does not seem appropriate for the catheter ablation of ILVT. Furthermore, if the FT is the Pd substrate, stably placing the ablation catheter at the middle portion of the FT could be challenging. Therefore, the target for catheter ablation should be set at the distal Pd site fused with the Pp potential, at which the latest Pd potential connects to the earliest Pp potential. In our proposed mechanism of ILVT, the reentry circuit includes the PPM itself, although this depends on the location of the FT. If the FT running between the PPM and LV septum is responsible for the ILVT, the PPM is considered to be a part of the reentry circuit and the PPM-FT conduction might also be critical to the perpetuation of tachycardia. This is consistent with a recent clinical finding that ILVT can be cured by RF application to the PPM [21].

#### 4.5. Study limitations

This study has several limitations. First, we did not apply any programmed pacing to entrain the tachycardia in order to avoid interruptions to the tachycardia. In this study, our main purpose was to delineate the 3-D mapping of the Pd and Pp potentials. Second, due to mechanical bumps during the manipulation of the mapping catheter, the mapping procedures (1st protocol) were sometimes suspended. However, we ultimately completed the mapping in all cases by waiting for the disappearance of the bump effect under the continuous administration of isoproterenol. Third, the presence of the FT was not investigated by echocardiography in the 6 patients included in the 1st protocol. Conversely, precise Pd mapping was not performed in the 2 patients included in the 2nd protocol. Finally, the local electrogram was not recorded along the entire FT according to its running length in the 2nd

protocol. Therefore, we could not obtain definitive proof that the entire FT was involved in the critical part of the reentry circuit.

#### Acknowledgments

The authors express special gratitude to Mr. John Martin for his linguistic assistance.

#### References

- [1] Belhassen B, Rotmensch HH, Laniado S. Response of recurrent sustained ventricular tachycardia to verapamil. *Br Heart J* 1981;46:679–82.
- [2] Ohe T, Shimomura K, Aihara N, et al. Idiopathic sustained left ventricular tachycardia: clinical and electrophysiological characteristics. *Circulation* 1988;77:560–8.
- [3] Wen MS, Yeh SJ, Wang CC, Lin FC, Wu D. Successful radiofrequency ablation of idiopathic left ventricular tachycardia at a site away from the tachycardia exit. *J Am Coll Cardiol* 1997;30:1024–31.
- [4] Tsuchiya T, Okumura K, Honda T, et al. Significance of late diastolic potential preceding Purkinje potential in verapamil-sensitive idiopathic left ventricular tachycardia. *Circulation* 1999;99:2408–13.
- [5] Nogami A, Naito S, Tada H, et al. Demonstration of diastolic and presystolic Purkinje potentials as critical potentials in a macroreentry circuit of verapamil-sensitive idiopathic left ventricular tachycardia. *J Am Coll Cardiol* 2000;36:811–23.
- [6] Aiba T, Suyama K, Aihara N, et al. The role of Purkinje and pre-Purkinje potentials in the reentrant circuit of verapamil-sensitive idiopathic LV tachycardia. *Pacing Clin Electrophysiol* 2001;24:333–44.
- [7] Maruyama M, Tadera T, Miyamoto S, Ino T. Demonstration of the reentrant circuit of verapamil-sensitive idiopathic left ventricular tachycardia: direct evidence for macroreentry as the underlying mechanism. *J Cardiovasc Electrophysiol* 2001;12:968–72.
- [8] Ouyang F, Cappato R, Ernst S, et al. Electroanatomic substrate of idiopathic left ventricular tachycardia: unidirectional block and macroreentry within the Purkinje network. *Circulation* 2002;105:462–9.
- [9] Chu J, Sun Y, Zhao Y, et al. Identification of the slow conduction zone in a macroreentry circuit of verapamil-sensitive idiopathic left ventricular tachycardia using electroanatomic mapping. *J Cardiovasc Electrophysiol* 2012;23:840–5.
- [10] Miyauchi Y, Kobayashi Y, Ino T, Atarashi H. Identification of the slow conduction zone in idiopathic left ventricular tachycardia. *Pacing Clin Electrophysiol* 2000;23:481–7.
- [11] Lotkowski D, Grzybiak M, Kozłowski D, et al. A microscopic view of false tendons in the left ventricle of the human heart. *Folia Morphol (Warsz)* 1997;56:31–9.
- [12] Abdulla AK, Frustaci A, Martinez JE, et al. Echocardiography and pathology of left ventricular “False Tendons”. *Chest* 1991;98:129–32.
- [13] Thakur RK, Klein GJ, Sivaram CA, et al. Anatomic substrate for idiopathic left ventricular tachycardia. *Circulation* 1996;93:497–501.
- [14] Lin FC, Wen MS, Wang CC, et al. Left ventricular fibromuscular band is not a specific substrate for idiopathic left ventricular tachycardia. *Circulation* 1996;93:525–8.
- [15] Luetmer PH, Edwards WD, Seward JB, et al. Incidence and distribution of left ventricular false tendons: an autopsy study of 483 normal human hearts. *J Am Coll Cardiol* 1986;8:179–83.
- [16] Nakagawa H, Beckman KJ, McClelland JH, et al. Radiofrequency catheter ablation of idiopathic left ventricular tachycardia-guided by Purkinje potential. *Circulation* 1993;88:2607–17.
- [17] The reply to a letter to the editor; Papillary muscle hypothesis of idiopathic left ventricular tachycardia (Chen PS, Karagueuzian HS). *J Am Coll Cardiol* 2001;37:1476.
- [18] Joyner RW, Ramza BM, Tan RC. Effects of stimulation frequency on Purkinje-ventricular conduction. *Ann NY Acad Sci* 1990;591:38–50.
- [19] Kim YH, Xie F, Yashima M, et al. Role of papillary muscle in the generation and maintenance of reentry during ventricular tachycardia and fibrillation in isolated swine right ventricle. *Circulation* 1999;100:1450–9.
- [20] Kaneko Y, Taniguchi Y, Nakajima T, Manita M, Ito T, Akiyama M, Kurabayashi M. Myocardial bundles with slow conduction properties are present on the left interventricular septal surface of normal human heart. *J Cardiovasc Electrophysiol* 2004;15:1010–8.
- [21] Park J, Kim YH, Hwang C, Pak HN. Electroanatomical characteristics of idiopathic left ventricular tachycardia and optimal ablation target during sinus rhythm: significance of preferential conduction through Purkinje fibers. *Yonsei Med J* 2012;53:279–88.